NONEQUILIBRIUM VELOCITY DISTRIBUTION OF REACTIVE FOREIGN GAS: SIMULATION AND PHENOMENOLOGY*

B. NOWAKOWSKI[a,b] AND J. GORECKI[a]

[a]Institute of Physical Chemistry, Polish Academy of Sciences
PL-01-224 Warsaw, Kasprzaka 44/52, Poland
[b]Department of Physics, Warsaw Agricultural University
Rakowiecka 28, 02-528 Warsaw, Poland

(Received January 3, 1996)

The velocity distribution function of a homogeneous foreign gas reacting with a carrier gas is studied by means of the Monte Carlo simulation and it is calculated using an approximate phenomenological approach assuming the Maxwellian form of the distribution with nonequilibrium temperature. The transition of the system to the hydrodynamic regime is demonstrated. The effect of the chemical reaction on the distribution function is presented in terms of decrease in the second and fourth moments of the velocity distribution for a wide range of activation energies and ratios of molecular masses. Good agreement between the results of Monte Carlo simulations and the approximate calculations is observed.

PACS numbers: 82.20. Db, 82.20. Mj

1. Introduction

Deformation of equilibrium velocity distribution due to a chemical reaction is a recognized problem of the kinetic theory [1] which has regained considerable interest in the last years [2]. The perturbation of the equilibrium Maxwellian is caused by a selective depletion of more energetic reactant molecules by the chemical process. Both kinetic theory [3–6] and numerical simulations [7–9] were applied to describe these nonequilibrium effects for a variety of reactive systems. In this work we study a homogeneous system

* Presented at the VIII Symposium on Statistical Physics, Zakopane, Poland, September 25–30, 1995.

consisting of a foreign (trace) gas A diluted in a carrier gas C, which are involved in an irreversible reaction

$$A + C \rightarrow \text{ products (neglected)}$$

Under the condition $n_A/n_C \ll 1$ for number concentrations of the species, it can be assumed that the perturbation of the equilibrium state of the carrier gas by the chemical process is negligible. The distribution function $f(v,t)$ of velocity v of the spatially uniform foreign gas is governed by the linear Boltzmann–Lorentz equation

$$\frac{\partial f}{\partial t} = \int \left(f_C'^{(0)} f' - f_C^{(0)} f \right) |\boldsymbol{v} - \boldsymbol{v}_C| d\sigma d\boldsymbol{v}_C - \int f_C^{(0)} f |\boldsymbol{v} - \boldsymbol{v}_C| d\sigma^* d\boldsymbol{v}_C \,, \quad (1)$$

where $f_C^{(0)}$ denotes the equilibrium velocity distribution of the carrier gas. The first term of the right hand side of Eq. (1) accounts for elastic $A - C$ collisions with the cross section $d\sigma$, and the second one for reactive collisions with the cross section $d\sigma^*$, respectively. The foreign gas system is a widely studied model in the kinetic theory [10], and contains two important special cases obtained as the ratio of molecular masses m_A/m_C tends to extremes: in the limit $(m_A/m_C)^{1/2} \ll 1$ one recovers the Lorentz gas, while the opposite Brownian regime, $(m_A/m_C)^{1/2} \gg 1$, leads to the model of Rayleigh gas.

As Eq. (1) admits the separation of variables, the time dependence of a solution of kinetic equation (1) is determined by the set of (negative) eigenvalues of the self-adjoint collision operator. For nonreactive system, it is well known that the maximum eigenvalue is separated from the rest of the spectrum, which consists of a few discrete eigenvalues over the threshold of continuum covering the remainder of the negative semi-axis [10, 11]. If the rate of reaction is not excessively high, these basic features of the spectrum should extend to the reactive system. In the long time limit the prevailing contribution to $f(v,t)$ is provided by the single eigenfunction $\phi(v)$ corresponding to the maximum eigenvalue α. The system described by Eq. (1) attains then the hydrodynamic regime, in which the concentration of species A diminishes at a constant rate, but the shape of velocity distribution tends to a definite stationary form

$$f(v,t) \simeq N \exp(\alpha t)\phi(v) \qquad \begin{pmatrix} \text{hydrodynamic} \\ \text{regime} \end{pmatrix} . \quad (2)$$

Outside the hydrodynamic regime the form of the velocity distribution is not universal and depends also on initial conditions, as several modes contribute to f.

Eq. (1) has been solved numerically by calculating approximately the eigenfunctions expanded in the first six Sonine polynomials [12]. However, this relatively limited representation for f can hardly be expected to reproduce the complex structure of the spectrum containing the infinite continuum part. Moreover, it was found that expansion in Sonine polynomials is inadequate and slowly convergent [11, 13] especially in the Lorentz range, which will turn out to constitute the important case of the system studied. In spite of the limited accuracy of the higher eigenvalues obtained by the applied numerical solution, it was rather the non-hydrodynamic regime that attracted primary interest in Ref. [12]. On the contrary, in the present work we confine our attention to the hydrodynamic stage of evolution.

For relatively slow chemical processes Eq. (1) has been solved [14] by the perturbative method. On the other hand, a simple phenomenological approach proposed lately [6, 15, 16] has been found to agree well with molecular dynamics and Monte Carlo (MC) simulations of reactive system $A + A \rightarrow B + B$, even for fast reactions with low activation energies. It assumes the Maxwellian form of distribution functions of the reactants, but because of the chemical reaction the temperatures of various species are different.

The case of reactive Lorentz gas has been studied in some detail [17] by means of the differential equation derived from the Boltzmann equation (1) in the limit $m_A/m_C \ll 1$. The accurate numerical solution of the differential form of Eq. (1) has been carried out and used to determine conditions in which the perturbative result for the chemical Boltzmann equation applies. However, for the Lorentz gas a process of relaxation of velocity distribution by elastic collisions is inefficient [12, 14], and the range of validity of the perturbation solution of Eq. (1) is relatively more restricted.

In this paper we present results of Monte Carlo simulations for the nonequilibrium effects in the system defined above. In Section 2 the specific numerical method is developed to study the foreign gas in the thermal bath. The standard molecular dynamics method is not effective for this ensemble, because much of computational effort is wasted to simulate the large thermal reservoir. The presented approach treats the collision stochastics more rigorously than the Bird method, usually applied in gas dynamics simulations. In Section 3 we present the approximate phenomenological approach, assuming the Maxwellian form of the distribution function. The results obtained by the simulations and the approximate calculations are presented and discussed in Section 4. The results of this paper are also compared with the perturbative solution of Eq. (1).

2. Method of Monte Carlo simulations

As the A molecules do not interact with each other, it is sufficient to consider only one-particle dynamics. A motion of a single A molecule consists of a sequence of free flights, interrupted by collisions with molecules of the carrier C. The collisions may be either elastic or reactive, in the latter case terminating the motion since products are neglected. The collision is assumed reactive with the probability s_f (steric factor) if it satisfies the following condition for velocities

$$\boldsymbol{e} \cdot (\boldsymbol{v} - \boldsymbol{v}_C) \geq g \,. \tag{3}$$

Here $\boldsymbol{e}$ denotes the unit vector along the line connecting the centers of molecules A and C at the instant of impact, and g is the threshold relative velocity, which determines the energy barrier of reaction

$$E = \tfrac{1}{2}\mu g^2 \,, \tag{4}$$

where μ denotes the reduced mass, $\mu = m_A m_C/(m_A + m_C)$. Otherwise the collision is elastic, and it follows the hard spheres dynamics.

The motion of an A molecule can be generated, if *(i)* the statistics of the free flights is determined, and *(ii)* the rule for a stochastic change in velocity in a collision is established. Let us consider a molecule moving with velocity $\boldsymbol{v}$ through the carrier C. For the assumed equilibrium velocity distribution of C at temperature T,

$$f_C^{(0)}(v_C) = n_C \,(m_C/2\pi kT)^{3/2} \exp\left(m_C v_C^2/2kT\right) \,, \tag{5}$$

the collision rate for the A molecule can be calculated as

$$\begin{aligned} \nu(v) &= \pi d_{AC}^2 \int f_C^{(0)}(v_C)|\boldsymbol{v} - \boldsymbol{v}_C| d\boldsymbol{v}_C \\ &= n_C \pi d_{AC}^2 \sqrt{\frac{2kT}{\pi m_c}} \left(\exp(-u^2) + \left(2u + \frac{1}{u}\right) \operatorname{erf}(u)\right) \,, \end{aligned} \tag{6}$$

where $d_{AC} = \frac{1}{2}(d_A + d_C)$ is the collisional diameter, and $u = v(m_C/2kT)^{1/2}$. The unnormalized error function in (6) is defined by

$$\operatorname{erf}(x) = \int_0^x \exp(-y^2) dy \,. \tag{7}$$

The distribution of collision waiting times τ for the A molecule is exponential

$$\theta_v(\tau) = \nu(v) \exp\left(-\nu(v)\tau\right) \,, \tag{8}$$

which also provides the distribution of times of free flight for a given velocity v. The free motion is terminated by a collision with a molecule C, and according to Eq. (1) the normalized distribution of velocity $\boldsymbol{v}_C$ of random collision partner is given by

$$W_{\boldsymbol{v}}(\boldsymbol{v}_C) = \frac{\pi d_{AC}^2}{\nu(v)} f_C^{(0)}(\boldsymbol{v}_C)|\boldsymbol{v} - \boldsymbol{v}_C| \,. \tag{9}$$

A geometry of collision is determined by e, which is specified by a point of uniform distribution on the circular target of total (elastic and reactive) cross section πd_{AC}^2 .

Using the above results we are in a position to provide the algorithm for simulation. At the beginning a molecule of A is generated with a velocity $\boldsymbol{v}$ chosen from the Maxwellian distribution at the temperature T of the carrier gas. The next steps are as follows:

1. calculating the collision rate $\nu(v)$ and choosing a time of free flight τ from distribution (8)
2. choosing a velocity $\boldsymbol{v}_C$ of collision partner from distribution (9), and a point of impact from the uniform distribution on the area of the total cross section
3. checking condition (3) for reactive collision, if satisfied the motion of the molecule is terminated
4. in case of elastic collision, the postcollisional velocity $\boldsymbol{v}'$ of the molecule A is calculated
5. return to step 1.

Motion of the molecule is followed until either it undergoes a reactive collision or the pre-defined time limit is reached, which is discussed in more detail below. Then a next molecule is generated and so on, until a desired accuracy of statistics is obtained.

It is readily checked that for the equilibrium nonreactive ensemble the transition rates in this Monte Carlo method satisfy the detailed balance condition. Let the molecule A changes its velocity from $\boldsymbol{v}$ to $\boldsymbol{v}'$ in the collision which transforms $\{\boldsymbol{v}, \boldsymbol{v}_C\}$ into $\{\boldsymbol{v}', \boldsymbol{v}_C'\}$ under the appropriate geometry e. The rate of transition along this path can be composed as

$$\Pi(\boldsymbol{v} \to \boldsymbol{v}'; \boldsymbol{v}_C, e) = \nu(v) W_{\boldsymbol{v}}(\boldsymbol{v}_C) \left(\pi d_{AC}^2\right)^{-1} = f_C^{(0)}(\boldsymbol{v}_C)|\boldsymbol{v} - \boldsymbol{v}_C| \,. \tag{10}$$

The inverse elastic collision yields $\{\boldsymbol{v}, \boldsymbol{v}_C\}$ from $\{\boldsymbol{v}', \boldsymbol{v}_C'\}$, in the geometry given by $-e$.

Combining Eq. (10) with the equilibrium Maxwellian distribution of A, $f^{(0)}$ given by Eq. (5) with the obvious replacements, one finds the relation

$$\begin{aligned} f^{(0)}(v)\Pi(\boldsymbol{v} \to \boldsymbol{v}'; \boldsymbol{v}_C, \boldsymbol{e}) &= f^{(0)}(v) f_C^{(0)}(v_C)|\boldsymbol{v} - \boldsymbol{v}_C| \\ &= f^{(0)}(v') f_C^{(0)}(v'_C)|\boldsymbol{v}' - \boldsymbol{v}'_C| \\ &= f^{(0)}(v')\Pi(\boldsymbol{v}' \to \boldsymbol{v}; \boldsymbol{v}'_C, -\boldsymbol{e}) \end{aligned} \tag{11}$$

In Eq. (11) it was used that the total kinetic energy and the absolute value of relative velocity are conserved in elastic collisions. Summing up relation (11) over paths with all possible $\boldsymbol{v}_C$ and $\boldsymbol{e}$, one recovers the detailed balance principle for the total transition rate

$$f^{(0)}(v)\Pi(\boldsymbol{v} \to \boldsymbol{v}') = f^{(0)}(v')\Pi(\boldsymbol{v}' \to \boldsymbol{v}). \tag{12}$$

Eq. (12) is not satisfied for a system with irreversible reaction, because there are no reverse transitions which could balance reactive collisions leading to products. For this system the actual equilibrium state does not exist.

Since early Monte Carlo attempts in gas dynamics [18] it has been realized that the stochastics of collisions is generated by the kernel of the collision integral of kinetic equation. It is the advantage of linear Eq. (1) that it yields the distribution $W_{\boldsymbol{v}}(\boldsymbol{v}_C)$ given by Eq. (9), which is determined by the given equilibrium distribution $f_C^{(0)}$ of the carrier gas. The MC simulation of the foreign gas is driven by the quasi external factor, that is the interaction with the gas C treated as a random medium. For this reason, the presented method resembles the simulation of the chemical master equation [19], which is also linear with respect to the distribution function. In reference to simulation methods developed in the context of the kinetic theory, the approach of this paper is related to the method of Koura [20] elaborated for the regular nonlinear Boltzmann equation. However, for mixtures with more balanced component concentrations the collision frequency ν involves the unknown distribution function f itself. Due to this coupling, in the exact implementation of this method recalculation of ν after each single collision (numerically, as f is tabulated) creates an enormous computational overload. To make the method practically applicable, the approximation was proposed to calculate ν in finite time intervals [20]. As another Monte Carlo approach, the method developed by Bird [21] has been proved to be more efficient in treatment of complex flows, although it handles the collision statistics in a more approximate way.

The simulated ensemble contains initially of the order of 10^6 molecules A generated with the Maxwellian velocity distribution at temperature T. After a finite lapse of time, the transient term of the distribution function

decays and the system reaches the hydrodynamic regime, in which the velocity distribution acquires the stationary form given by Eq. (2). Thus, the time range of the simulation should exceed the initial transient period and cover the stationary regime. The time of decay of the transient term corresponding to the higher eigenfunctions can be evaluated by means of the second largest eigenvalue of the collision operator. We approximated this decay rate using the numerical results for the eigenvalues of the operator of Eq. (1) for the nonreactive system [11]. After the hydrodynamic regime is reached, the simulation is continued for the period of time necessary to obtain a few independent samples of the system taken at equidistant time instants. The results obtained at the consecutive instants are considered independent, if they are separated by the time interval related to the velocity decorrelation time, evaluated on the basis of the diffusion coefficient.

3. Phenomenological approximation

Recent molecular dynamics simulations of model thermally activated reactions in an adiabatic system of hard spheres suggest that the velocity distribution functions of reagents may be approximated by the Maxwellian distributions with temperatures which are specific for each of the species [9, 15]. This assumption means that

$$f(v,t) = n_A \left(m_A/2\pi k T_A\right)^{3/2} \exp\left(-m_A v^2/2kT_A\right) , \tag{13}$$

where n_A and T_A are the time dependent concentration and temperature of A, respectively. Inserting ansatz (13) into the Boltzmann equation (1), after integration over $\boldsymbol{v}$ one obtains the macroscopic kinetic equation for the concentration n_A

$$\frac{dn_A}{dt} = \alpha(T_A) n_A , \tag{14}$$

where the rate constant α is a function of the temperature T_A

$$\alpha(T_A) = -s_f n_C \pi d_{AC}^2 \left(\frac{8k(T_A m_C + T m_A)}{\pi m_A m_C}\right)^{1/2} \exp\left(\frac{E(m_A+m_C)}{k(T_A m_C + T m_A)}\right) . \tag{15}$$

Equation (14) for the chemical kinetics is consistent with form (2) of the distribution function in the hydrodynamic regime. A closed set of equations for the parameters of distribution (13) is obtained by complementing Eq. (14) by the equation for T_A. The kinetic equation for this temperature is easily derived with the use of the density of kinetic energy, which for distribution function (13) is equal to $\frac{3}{2} n_A k T_A$. Multiplying the Boltzmann

equation by $\frac{1}{2}m_A v^2$ and integrating over $\boldsymbol{v}$ one gets

$$\begin{aligned}
&\frac{3}{2}\frac{d}{dt}n_A kT_A \\
&= n_C \pi d_{AC}^2 \left(\frac{8k(T_A m_C + T m_A)}{\pi m_A m_C}\right)^{1/2} \frac{4m_A m_C}{(m_A + m_C)^2} n_A k(T - T_A) \\
&+ \alpha(T_A)\frac{4m_A m_C}{(m_A + m_C)^2}\left(1 + \frac{E(m_A + m_C)}{k(T_A m_C + T m_A)}\right) n_A k(T - T_A) \\
&+ \alpha(T_A)\left(\frac{3}{2} + \frac{T_A m_C}{2(T_A m_C + T m_C)} + \frac{E(m_A + m_C)T_A m_C}{k(T_A m_C + T m_A)^2}\right) n_A k T_A .
\end{aligned} \tag{16}$$

Macroscopic kinetic equations (14) and (16) can also be founded on a simple phenomenology, without resort to the Boltzmann equation [9, 16]. Eq. (16) is readily transformed into the equation for the temperature T_A . Using Eq. (14) one obtains after some simple algebra

$$\begin{aligned}
&\frac{dT_A}{dt} = \frac{2}{3} n_C \pi d_{AC}^2 \left(\frac{8k(T_A m_C + T m_A)}{\pi m_A m_C}\right)^{1/2} \frac{4m_A m_C}{(m_A + m_C)^2}(T - T_A) \\
&\times \left[1 - s_f\left(1 + \frac{E(m_A + m_C)}{k(T_A m_C + T m_A)}\right)\exp\left(-\frac{E(m_A + m_B)}{k(T_A m_C + T m_A)}\right)\right] \\
&+ \frac{2}{3}\alpha(T_A) T_A \left(\frac{T_A m_C}{2(T_A m_C + T m_A)} + \frac{E(m_C + m_A)T_A m_C}{k(T_A m_C + T m_A)^2}\right) .
\end{aligned} \tag{17}$$

Eqs. (14) and (17) can be simplified by introducing the dimensionless time, $t' = |\alpha(T)|t/s_f$, the scaled concentration

$$\rho = n_A/n_A(t = 0) , \tag{18}$$

and the relative change in the temperature of A

$$\vartheta = (T_A - T)/T . \tag{19}$$

For the variables ρ and ϑ the set of kinetic equations reads

$$\frac{d\rho}{dt'} = -s_f(\vartheta M_C + 1)^{1/2} \exp\left(\varepsilon \frac{\vartheta M_C}{\vartheta M_C + 1}\right)\rho , \tag{20}$$

$$\begin{aligned}
\frac{d\vartheta}{dt'} = &-\frac{8}{3}(\vartheta M_C + 1)^{1/2} M_A M_C \exp(\varepsilon)\vartheta \\
&\times \left[1 - s_f\left(1 + \frac{\varepsilon}{\vartheta M_C + 1}\right)\exp\left(-\frac{\varepsilon}{\vartheta M_C + 1}\right)\right] \\
&- \frac{2}{3} s_f(\vartheta M_C + 1)^{1/2} \exp\left(\varepsilon \frac{\vartheta M_C}{\vartheta M_C + 1}\right)(1 + \vartheta)^2 \\
&\times \left(\frac{M_C}{2(\vartheta M_C + 1)} + \frac{\varepsilon M_C}{(\vartheta M_C + 1)^2}\right) ,
\end{aligned} \tag{21}$$

where

$$\varepsilon = E/kT \tag{22}$$

is the dimensionless activation energy, and

$$M_A = \frac{m_A}{m_A + m_C}, \qquad M_C = \frac{m_C}{m_A + m_C}. \tag{23}$$

The set of equations (20, 21) can be solved numerically for any values of the parameters of the system and provides n_A and T_A as functions of time. Equation (21) is independent from Eq. (20) and thus the dynamics of temperature does not depend on the concentration of the reagent A. There is always a stable stationary state of ϑ in the interval $(-1, 0)$, because the right hand side of Eq. (21) is positive for $\vartheta = -1$ and it is negative for $\vartheta = 0$. Therefore, if in the initial state the temperatures of both species are equal, then T_A will always decrease and in the steady state it will be lower than T.

4. Results and discussion

Figures 1A,B present two examples of $\vartheta(t)$ plotted *vs.* $\rho(t)$ calculated from phenomenological equations (20), (21) and obtained from the average kinetic energy of particles in the MC simulations. The initial decrease of both ϑ and ρ in the transient regime is followed by the transition to the hydrodynamic regime, in which ϑ reaches the asymptotic stationary value. The simple phenomenology gives a correct quantitative description of the time evolution of ϑ. Let us notice that the difference between the stationary ϑ observed in the simulations and the steady state solution of Eq. (21) may be positive or negative, depending on parameters of reaction.

The normalized distribution of speed $v = |v|$ obtained in the steady state by the MC simulations is compared in Fig. 2 with the Maxwellian form of $4\pi v^2 f(v)$, using f given by Eq. (13). For the reagents of equal masses, $M_A = 0.5$, the agreement between the MC results and phenomenology is very good , and can be related to the coincidence of the respective temperatures ϑ for this system presented in Fig. 1A. In the case of disparate masses, $M_A = 0.01$, the curves are shifted apart, but it seems that Maxwellian with the temperature slightly higher than T_A obtained from the phenomenology provides a good approximation for the shape of the distribution resulted from the simulation (*cf.* the difference of ϑ for this system in Fig. 1B). Let us notice (Figs. 1) that in the latter case the decrease in ϑ is by an order of magnitude larger than for $M_A = 0.5$.

Figure 3 presents the stationary ϑ obtained by the simulations and phenomenology as a function of the ratio of molecular masses m_A/m_C, for

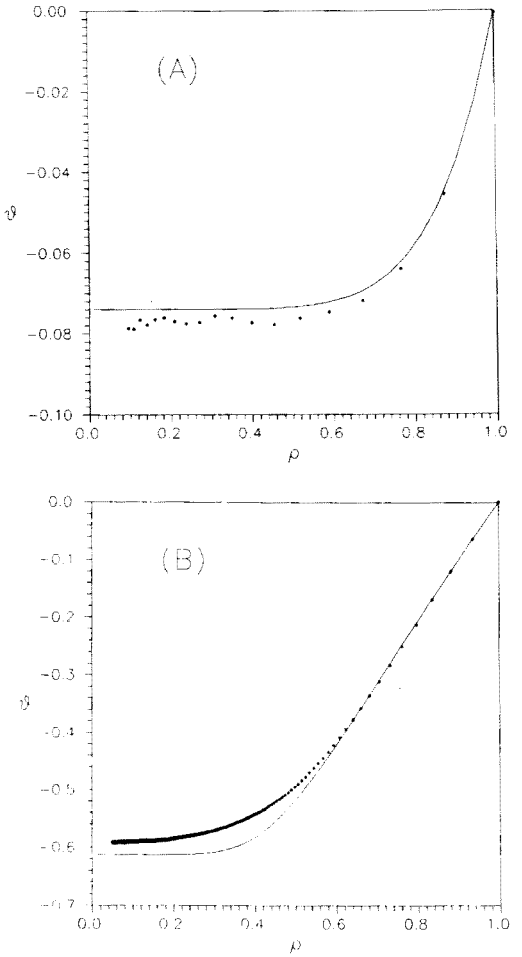

Fig. 1. ϑ as a function of ρ for the system in which the initial temperatures of components A and C are equal. The solid line corresponds to the numerical solution of Eqs.(20) and (21) , stars show results of the Monte Carlo simulations. (A) — $M_A = 0.5$, $s_f = 0.25$ and $\varepsilon = 1$. (B) — $M_A = 0.01$, $s_f = 0.25$ and $\varepsilon = 1$.

$\varepsilon = 1$ and the steric factors equal to 0.04 , 0.1 , and 0.25. Figure 4 shows the relative change in the fourth moment of the velocity distribution

$$Q = \frac{\langle v^4 \rangle - \langle v^4 \rangle_0}{\langle v^4 \rangle_0}, \tag{24}$$

where $\langle v^4 \rangle_0 = 15(kT)^2/m_A^2$ is the mean v^4 in the equilibrium ensemble, *i.e.* for Maxwellian with the unperturbed temperature T. The phenomenological

approximation using velocity distribution (13) yields

$$Q_{ph} = \frac{T_A^2 - T^2}{T^2}. \tag{25}$$

Good agreement between the MC simulations and phenomenology can be noticed in Figs. 3, 4. The results obtained in this paper are compared with the formulae derived by the perturbation method [14]

$$\vartheta = -\frac{1}{4M_A G}\left[G\left(\tfrac{1}{2}+\varepsilon\right) + \tfrac{1}{2}M_C^2\left(\tfrac{3}{4}+2\varepsilon-\varepsilon^2\right)\right] s_f \exp(-\varepsilon), \tag{26}$$

$$Q = -\frac{1}{2M_A G}\left[G\left(\tfrac{1}{2}+\varepsilon\right) - \tfrac{1}{2}M_A M_C\left(\tfrac{3}{4}+2\varepsilon-\varepsilon^2\right)\right] s_f \exp(-\varepsilon), \tag{27}$$

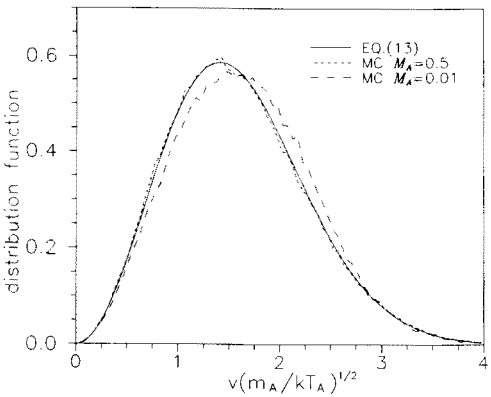

Fig. 2. The normalized distribution of speed $v = |\boldsymbol{v}|$. The solid line presents Maxwellian, Eq. (13); short dashed line — Monte Carlo simulations for $M_A = 0.5$, $s_f = 0.25$ and $\varepsilon = 1$; long dashed line — simulations for $M_A = 0.01$, $s_f = 0.25$ and $\varepsilon = 1$.

where $G = 5 - 6M_C + 7M_C^2$. The effects of the chemical reaction on both ϑ and Q exhibit a similar dependence on the ratio of masses m_A/m_C. It is most significant in the Lorentz limit, $m_A/m_C \to 0$, then diminishes as m_A/m_C increases. Such a dependence results from the competition between the relaxation process and the chemical reaction. The transfer of energy in elastic $A-C$ collisions is not effective if the masses of molecules A and C are significantly different. In terms of dynamics of velocity distribution, a time of elastic relaxation of nonequilibrium modes becomes longer (compared to a mean time of free flight) if the molecular masses of the reagents are disparate [11]. The mechanism of elastic scattering is then not enough efficient to restore the equilibrium velocity distribution perturbed by the chemical reaction. On the other hand however, the perturbation itself diminishes in

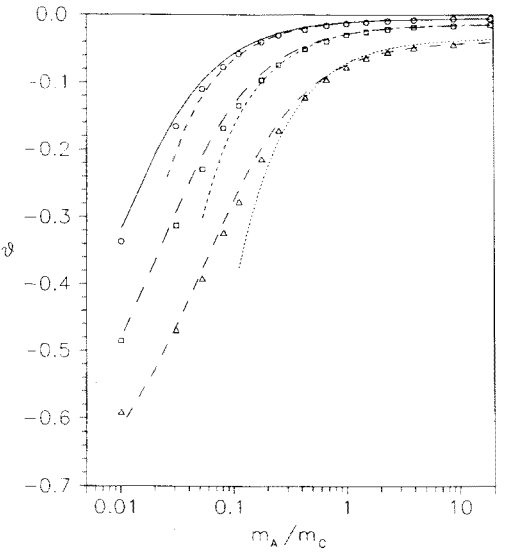

Fig. 3. ϑ as a function of m_A/m_C for $\varepsilon = 1$. Circles, squares and triangles indicate results of the MC simulations performed for $s_f = 0.04$, 0.1 and 0.25, respectively. The stationary values of ϑ calculated from phenomenological equation (21) for these successive steric factors are plotted using the solid, very long dashed and the long dashed lines. The medium dashed, short dashed and the dotted line present the perturbation result for ϑ, Eq. (26).

the Rayleigh limit, $m_A/m_C \to \infty$. In this range the condition for a reactive collision, Eq. (3), effectively does not involve the velocity v of the heavier molecule A. The reaction cross section becomes a constant, independent of a velocity of molecule A. Depletion of A by the reaction is uniform in the whole range of velocities, and the shape of the velocity distribution remains only slightly perturbed. Consequently, the corrections remain small even in the Rayleigh limit, $m_A \gg m_C$, although the relaxation process weakens. In conclusion, the dependence in Figs. 3, 4 follows from the fact that perturbation of the distribution function is the strongest in the Lorentz limit, and decreases if the system approaches the Rayleigh limit.

The results of Eqs. (26), (27) are confirmed by the MC data provided that reaction can be treated as a perturbation, that means effectively for not too small values of m_A/m_C. As the mass ratio approaches the Lorentz range the chemical reaction becomes stronger relative to the collisional relaxation and the perturbative solution is no longer valid. Accordingly, for $s_f = 0.04$ the perturbation curve diverges from the simulation results for $m_A/m_C < 0.05$, and for $s_f = 0.1$ and 0.25 this tendency begins already for higher m_A/m_C and is more pronounced. In the context of the numerical results [12], it was concluded that the perturbation method applies if the

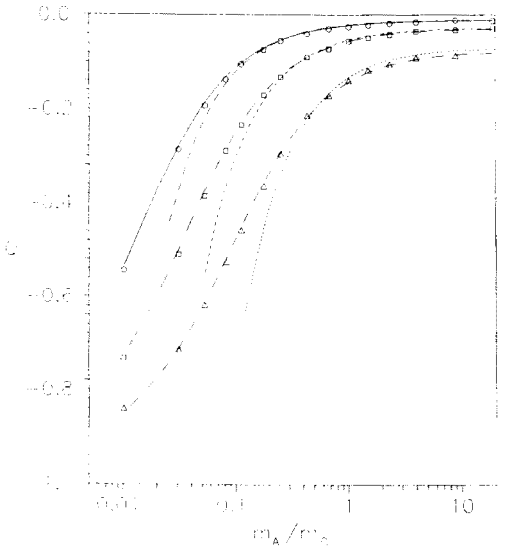

Fig. 4. Q as a function of m_A/m_C for $\varepsilon = 1$. Circles, squares and triangles indicate results of the MC simulations performed for $s_f = 0.04$, 0.1 and 0.25, respectively. Q_{ph} calculated from equation (25) using the stationary solution of phenomenological equation (21) for these successive steric factors are plotted using the solid, very long dashed and the long dashed lines. The medium dashed, short dashed and the dotted line present the perturbation result for Q , Eq. (27).

reaction rate constant is three orders of magnitude smaller than the rate of elastic collisions. However, this condition does not include a dependence on the mass ratio of reagents. On the contrary, our results prove that the range of validity of Eqs. (26), (27) is a very sensitive function of m_A/m_C, and this factor becomes even critical in the Lorentz range. While the MC data in Figs. 3, 4 indicate that the effects of the chemical reaction increase nonlinearly with s_f , perturbation equations (26), (27) predict respectively a simple linear dependence, which can be correct only for small probabilities s_f of reactive collision. Consequently, Figs. 3, 4 demonstrate that the range of validity of the perturbation result becomes more limited with increasing s_f.

Figure 5 presents the steady state of ϑ obtained by the MC simulations, phenomenology and the perturbation method as a function of the activation energy ε for $M_A = 0.05$ (close to the Lorentz limit) and the steric factors equal to 0.04, 0.1, and 0.25. Figure 6 shows the relative effect for Q , respectively. For both moments of the velocity distribution, the nonequilibrium effects of the chemical reaction exhibit a distinct extremum as a function of ε. The maximum effect can be observed at the activation energy $\varepsilon \leq 0.5$, and it tends towards smaller ε as s_f increases. For higher activation ener-

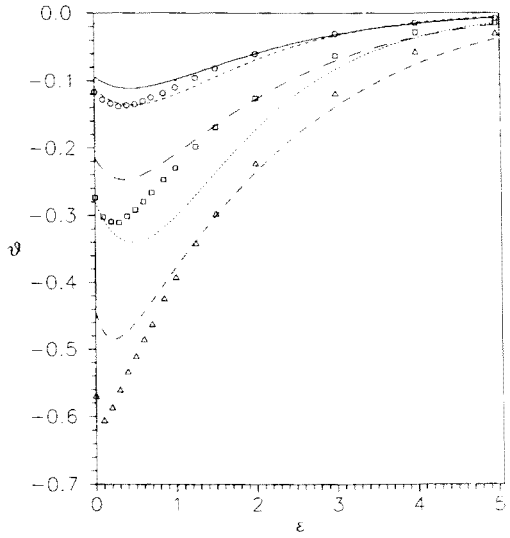

Fig. 5. ϑ as a function of ε for $M_A = 0.05$. Notation as in Figure 3.

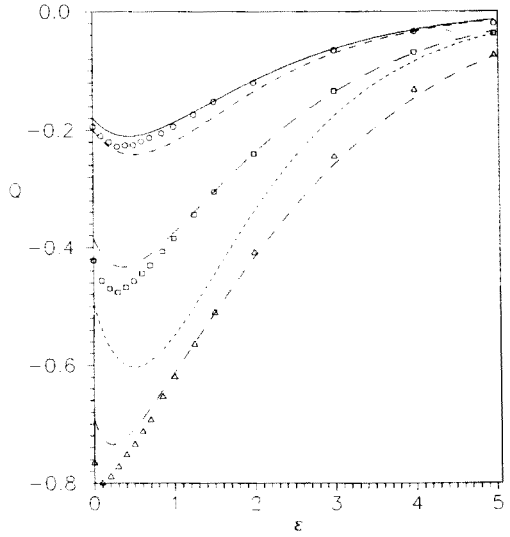

Fig. 6. Q as a function of ε for $M_A = 0.05$. Notation as in Figure 4.

gies the nonequilibrium effects decrease because reactive collisions become less frequent. On the other hand, for smaller ε molecules of A are depleted more uniformly from the whole range of velocities, so the perturbation of their distribution is weaker. The phenomenology gives accurate description of the effects on ϑ and Q except for the fastest reactions, for which $\varepsilon < 1$. Despite this discrepancy it correctly predicts the positions of the extrema.

In Figs. 5, 6 the agreement between the simulation data and the perturbation results is fairly good for the slowest reactions studied, $s_f = 0.04$. However, for the reactions with the steric factor $s_f = 0.1$ the difference between both results becomes significant, indicating that already in this case the reaction can hardly be treated as a perturbation. In the case of the highest steric factor studied, $s_f = 0.25$, the range of validity of perturbation result is even more limited, and therefore Eqs. (26), (27) for this value of s_f have not been plotted in Figs. 5, 6.

In the limit $s_f \to 0$ one obtains from Eq. (21) the following expression for the derivative of the stationary temperature

$$\frac{d\vartheta}{ds_f} = -\frac{1}{4M_A}\left(\frac{1}{2} + \varepsilon\right)\exp(-\varepsilon), \tag{28}$$

which can be used to calculate ϑ for small s_f . This expression reproduces the perturbative result obtained with the use of only the first Sonine polynomial (expansion in two Sonine polynomials is used in Eqs. (26), (27)).

We are not comparing our results with those of Ref. [12] because values of the moments of the velocity distribution are not given explicitly in that paper. Moreover, the numerical solution [12] was primarily oriented to study the transient regime. However, transient phenomena are beyond the scope of the present work.

In the paper we made no assumption concerned with a heat effect associated with the chemical reaction. The obtained results remain valid for moderately exothermic and endothermic processes, provided that $n_A \ll n_C$.

5. Conclusions

The method of Monte Carlo simulations of the system composed of the foreign trace gas reacting with the carrier gas has been proposed and applied to study the nonequilibrium effects. It provides the accurate results for the velocity distribution for a wide range of reaction parameters.

The simulations have confirmed that the concept of nonequilibrium temperature [9, 15, 16] may be useful to describe a distribution of energetic states of reagents. The phenomenological equations predict correctly the magnitude of the nonequilibrium effects. The Maxwellian distribution at the stationary temperature T_A calculated from the phenomenology is much closer to the real stationary velocity distribution than the Maxwellian with the temperature T of the carrier. Therefore, the use of the former distribution as the initial state of the foreign gas in the simulations can significantly shorten a time to reach the hydrodynamic regime of the nonequilibrium system, and consequently increase efficiency of the MC method. An additional advantage of the Maxwellian form of f is that it is more convenient for sample generation than other applicable distributions.

REFERENCES

[1] I. Prigogine, E. Xhrouet, *Physica* **15**, 913 (1949).
[2] *Cf.* a number of recent papers in *Far-from-Equilibrium Dynamics of Chemical Systems*, edited by J. Gorecki *et al.*, World Scientific, Singapore 1994.
[3] J. Ross, P. Mazur, *J. Chem. Phys.* **35**, 19 (1961).
[4] B. Shizgal, M. Karplus, *J. Chem. Phys.* **52**, 4262 (1970); *J. Chem. Phys.* **54**, 4345 (1971); *J. Chem. Phys.* **54**, 4357 (1971).
[5] N. Xystris, J.S. Dahler, *J. Chem. Phys.* **68**, 374 (1978).
[6] B.C. Eu, K.-W. Li, *Physica* **88A**, 135 (1977).
[7] J. Gorecki, *J. Chem. Phys.* **95**, 2041 (1991).
[8] J. Gorecki, J. Popielawski, A.S. Cukrowski, *Phys. Rev.* **A44**, 3791 (1991).
[9] J. Gorecki, B.C. Eu, *J. Chem. Phys.* **97**, 6695 (1992).
[10] M.R. Hoare, *Adv. Chem. Phys.* **20**, 135 (1971).
[11] C.S. Shapiro, N. Corngold, *Phys. Rev.* **137A**, 1686 (1965).
[12] B. Shizgal, *Chem. Phys.* **5**, 129 (1974).
[13] B. Shizgal, *J. Chem. Phys.* **70**, 1948 (1979); B. Shizgal, *Can. J. Phys.* **62**, 97 (1984).
[14] B. Nowakowski, J. Popielawski, *J. Chem. Phys.* **100**, 7602 (1994); B. Nowakowski, *Acta Phys. Pol.* **B26**, 1031 (1995).
[15] A.S. Cukrowski, J. Popielawski, L. Qin, J.S. Dahler, *J. Chem. Phys.* **97**, 9086 (1992).
[16] J. Gorecki, *J. Chem. Phys.* **98**, 7269 (1993).
[17] W. Stiller, R. Schmidt, J. Popielawski, A.S. Cukrowski, *J. Chem. Phys.* **93**, 2425 (1990).
[18] J.K. Haviland, in *Methods of Computational Physics* edited by B. Alder *et al.* vol.4, Academic Press, New York, 1965.
[19] D.T. Gillespie, *J. Phys. Chem.* **81**, 3240 (1977).
[20] K. Koura, *J. Chem. Phys.* **59**, 691 (1973).
[21] G.A. Bird, *Molecular Gas Dynamics*, Clarendon, Oxford 1976.